Discrete Event Approximation of Continuous Controllers

Ernesto Kofman

Laboratorio de Sistemas Dinamicos - FCEIA - Universidad Nacional de Rosario

Riobamba 245 bis - (2000) Rosario - Argentina

Email: kofman@fceia.unr.edu.ar

Abstract

This paper introduces Quantized-State Control, a method for the digital asynchronous implementation of controllers designed in continuous time. Through the quantization of its state and input variables the original continuous controller is mapped into a discrete event system within the DEVS formalism framework that can be implemented in a digital device.

It is shown that, under certain conditions, this implementation in general nonlinear systems approximately conserves the stability properties of the original continuous control system (CCS). A design algorithm is provided which allows to obtain a desired ultimate bound and region of attraction.

In the case of LTI systems, it is proven that the difference between the closed loop trajectories of both systems is always bounded by a constant which stands even in presence of any piecewise constant reference. The mentioned constant can be calculated by a closed formula which depends only on the system parameters and the quantization adopted.

Further advantages of the methodology are the improvement of the dynamic response and the reduction of the quantization effects of the converters and the computational costs with respect to classic discrete time implementations. These facts and the use of the design algorithm are illustrated through the simulation of different examples.

Keywords: Digital Control, Quantized Control, Discrete Event Systems, Asynchronous Control Systems.

1 Introduction

Practical implementations of most control systems require the use of digital devices. Due to the different nature of the signals present at the inputs and outputs of the digital controller and the continuous-time plant, the interconnection between them must be made through A/D and D/A converters.

On one hand, the classic A/D conversion techniques perform synchronous sampling leaving the plant without control between successive sample instants. This fact usually provokes a lost of performance in the dynamic response and affects the regions of attraction in nonlinear systems. This is due to the fact that a fixed sampling time which is adequate when the state is near an equilibrium point could be completely useless when the state is far away from that point.

On the other hand, the A/D conversions use only a finite number of bits producing undesirable effects such as steady state errors and oscillations.

Because of quantization problems attracting sets must be considered instead of equilibrium points, and *ultimate boundedness* of solutions instead of asymptotic stability. There are many works in the literature which study these quantization effects in linear systems –see (Miller et al., 1988; Miller et al., 1989; Farrel and Michel, 1989) for instance– which were also extended to nonlinear plants (Hou et al., 1997) and multirate control (Hu and Michel, 1999).

Instead of studying the effects of the quantization after the controller is designed, some works attempt to deal with the quantization at the design stage. In (Delchamps, 1990) the problem of stabilizing a discrete time linear system taking into account the quantization in the state measurement is studied. In (Brockett and Liberzon, 2000) there is also an study over CCS and the problem of the impossibility of convergence to the equilibrium points is solved by allowing the quantizers to change the size of the quantization intervals.

Since recently, quantization of variables is being applied for simulation purposes. In (Zeigler and Lee, 1998) the authors proposed that continuous time systems can be simulated through the quantization of some variables instead of the discretization of time. They also showed that the resulting system can be described by a discrete event model within the DEVS formalism (Zeigler et al., 2000).

This idea was taken in (Kofman and Junco, 2001), where the authors introduced the concept

of Quantized State System (QSS), that are continuous time systems where the state variables are quantized through hysteretic quantization functions. It has been shown that QSS with piecewise constant input trajectories can be exactly represented by DEVS models. Thus, the addition of the mentioned quantization functions to a continuous model transforms it into a QSS that can be simulated in a digital device.

The possibility of simulating DEVS models in real time (Zeigler and Kim, 1993) motivated the idea of using QSS as controllers and the definition of Quantized State Control (QSC), which was first introduced by the author in (Kofman, 2001). There, and making use of an asynchronous sampling technique described in (Sayiner et al., 1993), a control scheme is proposed where the time discretization is theoretically avoided.

In that way, QSC attacks simultaneously the both mentioned problems. On one hand, it does not leave the plant without control except when their outputs do not suffer significative modifications. On the other hand, QSC takes into account the quantization effects at the design stage allowing to reduce them to a desired bound.

The design of a QSC controller consists just in choosing the quantization to be applied at each state variable of a previously designed continuous controller as well as the quantization at the asynchronous converters. Then, an equivalent DEVS model can be easily found and digitally implemented.

In this work, we reformulate and extend the original definition of QSC and study their general properties in nonlinear and linear systems.

In the mentioned introductory paper, a theorem was presented showing that –under certain conditions– the QSC implementation of a continuous designed controller can ensure ultimately boundedness of the trajectories. Moreover, following an algorithm –which was given– it was possible to choose the quantization in order to achieve a desired ultimate bound and region of attraction of the CCS equilibrium point.

Here, we reformulate both, the theorem and the algorithm in order to arrive to less restrictive results allowing the use of the methodology also in time variying plants.

Then, the analysis is carried to the particular case of LTI systems where it is shown that the QSC system trajectories are always ultimately bounded (for any adopted quantization) provided that the CCS is asymptotically stable. Moreover, in that case it is proven that the trajectories

of the original CCS and the QSC cannot differ from each other in more than a given bound which can be calculated by a closed formula.

While for the nonlinear case the basic analysis tool consists in the Lyapunov theory, in the linear case we make use of a geometric study (Kofman, 2002) which allows arriving to a much less conservative result. The mentioned formula can be used to design the quantization according to the desired performance, replacing the Lyapunov-based algorithm deduced for the general nonlinear cases.

Finally, different examples of QSC in linear and nonlinear system are provided in order to illustrate the use of the design algorithm and formula and to show some advantages of the QSC methodology with respect to the classic discrete time implementation.

The paper is organized as follows: Section 2 recalls the principles of the Quantized State Systems. Then, the definition of QSC, the stability properties and the design algorithm are introduced in Section 3. Further, the particularization of the analysis for LTI systems is performed in Section 4 and finally Section 5 presents the mentioned examples.

2 Quantized State Systems

As it was already mentioned, QSS is based on the hysteretic quantization of the state variables. This quantization transforms the state trajectories into piecewise constant ones allowing the system representation in terms of the DEVS formalism.

Before giving the QSS definition, the concept of quantization function with hysteresis will be recalled

2.1 Quantization Functions

Definition 1. *Let $Q = \{Q_0, Q_1, ..., Q_r\}$ be a set of real numbers where $Q_{k-1} < Q_k$ with $1 \leq k \leq r$. Let Ω be the set of piecewise continuous real valued trajectories and let $x_i \in \Omega$ be a continuous*

trajectory. Let $b : \Omega \to \Omega$ *be a mapping and let* $q_i = b(x_i)$ *where the trajectory* q_i *satisfies:*

$$q_i(t) = \begin{cases} Q_m & \text{if } t = t_0 \\ Q_{k+1} & \text{if } x_i(t) = Q_{k+1} \wedge q_i(t^-) = Q_k \wedge k < r \\ Q_{k-1} & \text{if } x_i(t) = Q_k - \varepsilon \wedge q_i(t^-) = Q_k \wedge k > 0 \\ q_i(t^-) & \text{otherwise} \end{cases} \tag{1}$$

and

$$m = \begin{cases} 0 & \text{if } x_i(t_0) < Q_0 \\ r & \text{if } x_i(t_0) \geq Q_r \\ j & \text{if } Q_j \leq x(t_0) < Q_{j+1} \end{cases}$$

Then, the map b *is a* hysteretic quantization function.

The discrete values Q_k are called *quantization levels* and the distance $Q_{k+1} - Q_k$ is defined as the *quantum*, which is usually constant. The width of the hysteresis window is ε. The values Q_0 and Q_r are the lower and upper saturation bounds. Figure 1 shows a typical quantization function with uniform quantization intervals.

[Figure 1 about here.]

A fundamental property of a Quantization Function with hysteresis when $t \geq t_0$ and $Q_0 \leq x(t) \leq Q_r$ is given by the following inequality

$$|q(t) - x(t)| \leq \max_{1 \leq i \leq r} (Q_i - Q_{i-1}, \varepsilon) \tag{2}$$

2.2 Quantized State Systems

Consider the State Equation System given by:

$$\begin{cases} \dot{x}(t) &= f(x(t), u(t)) \\ y(t) &= g(x(t), u(t)) \end{cases} \tag{3}$$

Related to this system, an associated Quantized State System (Kofman and Junco, 2001) is defined as follows:

$$\begin{cases} \dot{x}(t) &= f(q(t), u(t)) \\ y(t) &= g(q(t), u(t)) \end{cases} \tag{4}$$

where $q(t)$ and $x(t)$ are related (componentwise) by quantization functions with hysteresis. The components of vector $q(t)$ are called *quantized variables.*

The most significant properties of QSS are related to the form of the trajectories. Provided that the inputs have piecewise constant trajectories and function f is continuous and bounded in any bounded domain, the following properties are satisfied:

- The quantized variables have piecewise constant trajectories
- The state variable derivatives have also piecewise constant trajectories
- The state variables have continuous piecewise linear trajectories

The accomplishment of these properties requires the use of hysteresis in the quantization. If non hysteretic –or memoryless– quantization were used, infinitely fast oscillations could occur and the resulting trajectories would not be piecewise constant or linear.

As a consequence of these properties the QSS can be exactly represented by a discrete event model within the DEVS formalism framework. The DEVS model related to a generic QSS, the proof of the mentioned properties and an extended explanation about the necessity of using hysteresis can be found in (Kofman and Junco, 2001).

It is interesting to mention here that DEVS allows to represent systems with an infinite number of possible states (the set of possible states could be $\Re^n$ for instance). In that way, it permits the representation and simulation of any QSS in a *deterministic* way, for any quantization adopted (provided that it is hysteretic). This fact contrasts with what happens when systems under quantization mesurement are represented by less general formalisms like Petri Nets or Finite Automata. In that case, the partition of the state–space should be made following special techniques in order to arrive to deterministic models (Lunze et al., 1999).

The possibility of representing a QSS by a DEVS model and the fact that DEVS models can be simulated in real time by digital devices[1] (Zeigler and Kim, 1993) suggest the use of QSS as digital controllers.

[1] DEVS representation of QSS is exact. However, real time simulation of DEVS has errors related to the temporal resolution and the round-off introduced by the digital device

3 Quantized State Control

3.1 QSC Definition

Consider the CCS consisting of plant and controller, Eqs. (5) and (6) respectively, and their (ideal) interconnection, Eq. (7).

$$\begin{cases} \dot{x}_p(t) &= f_p(x_p(t), u_p(t), t) \\ y_p(t) &= g_p(x_p(t), t) \end{cases} \tag{5}$$

$$\begin{cases} \dot{x}_c(t) &= f_c(x_c(t), u_c(t), u_r(t)) \\ y_c(t) &= g_c(x_c(t), u_c(t), u_r(t)) \end{cases} \tag{6}$$

$$u_p(t) = y_c(t), \quad u_c(t) = y_p(t) \tag{7}$$

Note that $u_r(t)$ represents an input reference.

Definition 2. *A QSS associated to a continuous controller* (6) *is called Quantized State Controller (QSC controller).*

Definition 3. *A QSC system is defined as a control scheme composed by a continuous plant and a QSC controller connected through asynchronous A/D and D/A converters.*

[Figure 2 about here.]

Figure 2 shows a block diagram representation of a QSC system. The QSC implementation of the controller transforms (6) into the new set of equations:

$$\begin{cases} \dot{x}_c(t) &= f_c(q_c(t), u_c(t), u_r(t)) \\ y_c(t) &= g_c(q_c(t), u_c(t), u_r(t)) \end{cases} \tag{8}$$

where the difference between the components of q_c and x_c is bounded according to (2).

The asynchronous sampling scheme (Sayiner et al., 1993) implies that the A/D conversions are performed only when the analog input and the digital output of the converters differ in a quantity corresponding to one quantization interval. Then, they can be seen as quantization functions with hysteresis where the quantization intervals and the hysteresis windows have the same size. In a similar way, the D/A converters can be represented by quantization functions

without hysteresis ($\varepsilon = 0$). Thus, the presence of the asynchronous converters transforms (7) into:

$$u_p(t) = y_{c_q}(t), \quad u_c(t) = y_{p_q}(t) \tag{9}$$

where the variables $y_{c_q}(t)$ and $y_{p_q}(t)$ are the quantized versions of the plant and the controller output variables, which differ componentwise from the continuous y_c and y_p in a quantity bounded by an inequality like (2).

3.2 Stability of QSC

The CCS closed loop equations can be derived from Equations (5)–(7) arriving to

$$\begin{cases} \dot{x}_p &= f_p(x_p, g_c(x_c, g_p(x_p, t), u_r), t) \\ \dot{x}_c &= f_c(x_c, g_p(x_p, t), u_r) \end{cases} \tag{10}$$

Let us define

$$\Delta x_c(t) = q_c(t) - x_c(t) \tag{11a}$$

$$\Delta y_p(t) = y_{p_q}(t) - y_p(t) \tag{11b}$$

$$\Delta y_c(t) = y_{c_q}(t) - y_c(t) \tag{11c}$$

Thus, from these definitions and Equations (5), (8) and (9), the QSC closed loop equations can be written as:

$$\begin{cases} \dot{x}_p &= f_p(x_p, g_c(x_c + \Delta x_c, g_p(x_p, t) + \Delta y_p, u_r) + \Delta y_c, t) \\ \dot{x}_c &= f_c(x_c + \Delta x_c, g_p(x_p, t) + \Delta y_p, u_r) \end{cases} \tag{12}$$

Then, the QSC system (12) can be seen as a perturbed version of the original CCS (10). Moreover, taking into account inequality (2) the perturbations in QSC are bounded componentwise by the corresponding quantum. This is true provided that the variables x_c, y_p and y_c do not reach the corresponding saturation bounds. From here to the end, it will be considered that the non–saturation region is enough large so that the trajectories do not leave it.

Based on this observation, the properties of the QSC implementation of a CCS can be studied by looking at the effects of bounded perturbations in the original closed loop system.

When the reference trajectory $u_r(t)$ is zero (or constant), the QSC system (12) can be rewritten as

$$\dot{x} = f(x + \Delta x, \Delta y, t) \tag{13}$$

where $x \triangleq [x_p, x_c]^T$, $\Delta x \triangleq [0, \Delta x_c]^T$, $\Delta y \triangleq [\Delta y_p, \Delta y_c]^T$, and $f \triangleq [f_p, f_c]^T$.

With these definitions, the CCS (10) becomes

$$\dot{x} = f(x, 0, t) \triangleq \tilde{f}(x, t) \tag{14}$$

Then, the following theorem which relates the stability properties of (14) and (13) can be stated:

Theorem 1. *Let the origin be an asymptotically stable equilibrium point of the closed loop CCS (14). Assume that function f is continuous and a continuously differentiable Lyapunov function $V(x,t)$ is known with*

$$W_1(x) \leq V(x,t) \leq W_2(x) \tag{15}$$

$$\frac{\partial V}{\partial x} \cdot \tilde{f}(x,t) + \frac{\partial V}{\partial t} \leq -W_3(x) \tag{16}$$

$\forall t \geq 0$, $\forall x \in D$ being D a compact set which contains the origin and W_i are continuous positive definite functions in D.

Let $\Omega_{2_a} = \{x | W_2(x) \leq a\}$ with a being an arbitrary positive constant which is enough small so that $\{x | W_1(x) \leq a\}$ is a closed region inside D.

Let $\Omega_{1_b} = \{x | W_1(x) \leq b\}$ being b an arbitrary positive constant ($b < a$) enough small so that $\Omega_{1_b} \subset \Omega_{2_a}$.

Then, a quantization can be found so that the QSC system trajectories starting in Ω_{2_a} finish inside Ω_{1_b}, reaching this region in finite time.

Proof. The derivative of $V(x,t)$ along the solutions of the QSC system (13) is

$$\begin{aligned} \dot{V}(x,t) &= \frac{\partial V}{\partial x} \cdot f(x + \Delta x, \Delta y, t) + \frac{\partial V}{\partial t} \\ &= \frac{\partial V}{\partial x} \cdot f(x, 0, t) + \frac{\partial V}{\partial t} + \frac{\partial V}{\partial x} \cdot (f(x + \Delta x, \Delta y, t) - f(x, 0, t)) \end{aligned}$$

Then, using (16) it results that

$$\dot{V}(x,t) \leq -W_3(x) + \frac{\partial V}{\partial x} \cdot (f(x + \Delta x, \Delta y, t) - f(x, 0, t)) \tag{17}$$

Consider the sets $\Omega_{2_b} = \{x | W_2(x) \leq b\}$ and $\Omega_{1_a} = \{x | W_1(x) \leq a\}$. From the hypotesis made about a and b, it results that

$$\Omega_{2_b} \subset \Omega_{1_b} \subset \Omega_{2_a} \subset \Omega_{1_a} \subset D \tag{18}$$

Since $W_3(x)$ is positive definite in D, it is positive in $\Omega_{1,2} \triangleq \Omega_{1_a} - \Omega_{2_b}$. Moreover, it exists a positive constant s where

$$s \triangleq \min_{x \in \Omega_{1,2}} W_3(x) \tag{19}$$

Let us define the following function

$$\alpha(x, \Delta x, \Delta y, t) \triangleq -W_3(x) + \frac{\partial V}{\partial x} \cdot (f(x + \Delta x, \Delta y, t) - f(x, 0, t)) \tag{20}$$

The continuity in functions W_3 and f and the fact that V is continuously differentiable implies that α is continuous. From the definition of α and Eq.(19) it results that

$$\alpha(x, 0, 0, t) \leq -s \;\; \forall x \in \Omega_{1,2}, \forall t \geq 0 \tag{21}$$

Let α_M be the function defined by

$$\alpha_M(\Delta x, \Delta y) \triangleq \sup_{x \in \Omega_{1,2}, t \geq 0} (\alpha(x, \Delta x, \Delta y, t)) \tag{22}$$

It can be easily seen that α_M is continuous and $\alpha_M(0, 0) \leq -s$. Then, for any positive number $s_1 < s$ a positive constant r can be found so that the condition

$$\|(\Delta x, \Delta y)\| \leq r \tag{23a}$$

implies that

$$\alpha_M(\Delta x, \Delta y) \leq -s_1 \tag{23b}$$

and then it results that

$$\dot{V}(x, t) \leq \alpha(x, \Delta x, \Delta y, t) \leq \alpha_M(\Delta x, \Delta y) \leq -s_1 \tag{24}$$

in $\Omega_{1,2}$.

From here to the end, the proof follows Theorem 5.3 of (Khalil, 1996).

Let $\Omega_{a,t} = \{x | V(x, t) \leq a\}$ and $\Omega_{b,t} = \{x | V(x, t) \leq b\}$ be time variable sets. From (15) it results that

$$\Omega_{2_b} \subset \Omega_{b,t} \subset \Omega_{1_b} \subset \Omega_{2_a} \subset \Omega_{a,t} \subset \Omega_{1_a} \subset D \tag{25}$$

The border of $\Omega_{a,t}$ is inside $\Omega_{1,2}$, where $\dot{V}(x, t)$ is negative. It means that the trajectories of the QSC system (13) cannot abandon $\Omega_{a,t}$.

Then, any trajectory starting in Ω_{2_a} cannot abandon Ω_{1_a}.

The border of $\Omega_{b,t}$ is also inside $\Omega_{1,2}$. Then the trajectories cannot abandon this time variable set.

To complete the proof, we need to ensure that the trajectories initiated in $\Omega_{2_a} \subset \Omega_{a,t}$ reach $\Omega_{b,t}$ in a finite time.

Let $\phi(t)$ be a solution of (13) starting in $\Omega_{a,t}$ (i.e. $V(\phi(0), 0) \leq a$) and let us suppose that

$$V(\phi(t), t) > b \ \ \forall t \tag{26}$$

then we have $\dot{V}(\phi(t), t) \leq -s_1$ and after

$$t_1 \triangleq \frac{a-b}{s_1} \tag{27}$$

it results that $V(\phi(t_1), t_1) \leq b$ which yields a contradiction. Then, the region $\Omega_{b,t}$ must be reached before the finite time t_1.

Since $\Omega_{b,t} \subset \Omega_{1_b}$ the trajectory also reaches the set Ω_{1_b} before that time. □

Equation (23a) gives the maximum perturbation allowed to ensure the achievement of the proposed goal (i.e. the region of attraction Ω_{2_a} and the ultimate bound in Ω_{1_b}). Since the maximum perturbation in each variable is given by the corresponding quantum, this equation should be used to choose the quantum at the different controller state variables and converters completing in that way the QSC design.

Observe that Ω_{2_a} is also the estimation of the region of attraction of the CCS using the Lyapunov function V. Then, a QSC implementation can be found so that it conserves the estimated region of attraction.

The presence of quantization destroyes the asymptotic stability. However, ultimately boundedness of the solutions can be still ensured. Moreover, the ultimate region Ω_{1_b} can be arbitrarily chosen. Anyway, if it is chosen to be too small then the quantum will also result too small and the computational costs will increase over what can be practically implemented since the rate of events in the controller is approximately proportional to the inverse of the quantum.

3.3 An algorithm for QSC implementation

The design of a QSC contoller can be divided in two steps. The first one is the design of the continuous controller, which can be done following any technique.

The second step is the choice of the quantization at each variable. The use of a very small quantum yields solutions which are very closed to the trajectories of the CCS. This is due to the property of convergence which tells that –under locally Lipchitz conditions on the functions– the solutions of the QSC system go to the solutions of the CCS when the quantization go to zero (Kofman, 2001). In that way, and also according to Theorem 1, the ultimate bound can be reduced to arbitrary small values.

However, as it was already mentioned, the use of a small quantum increases the number of events at the controller and the digital device can fail in its attempt to give the correct output values at the required time.

Therefore, there is always a trade–off between accuracy and practical considerations related to the computational costs. Then the idea is to exploit Theorem 1 in order to choose the quantization according to some essential features (region of attraction and ultimate bound). In that way, the quantization adopted will be just as small as necessary to ensure those properties and –provided that the CCS is not too fast– the digital device will be able to correctly implement the resulting QSC controller.

The translation of these ideas into a design algorithm for QSC can be written as follows:

1. Design a continuous controller and calculate the Lyapunov function $V(x,t)$ and the functions $W_i(x)$ according to (15)–(16) for the closed loop CCS.

2. Choose the QSC region of attraction Ω_{2_a} and the ultimate region Ω_{1_b} together with the constants a and b.

3. Obtain the perturbed closed loop function f according to (13).

4. Obtain function α according to (20) and α_M according to (22).

5. Calculate constant s according to (19) and choose the positive constant $s_1 < s$. If the goal is just to ensure ultimately boundedness s_1 should be very small. Otherwise, if the speed of convergence is also important, it can be chosen taking into account (27).

6. Compute the value of r according to (23).

7. Choose the quantization at the controller state variables and converters so that (23a) is satisfied.

It can be easily seen that this procedure leads to a QSC controller which ensures region of attraction Ω_{2_a} and ultimate region Ω_{1_b}.

4 QSC in LTI Systems

The analysis of Section 3 can be also applied to the particular case of linear time invariant systems.

However, the design algorithm is not very practical and its use can lead to conservative results. This is due to the fact that the Lapunov analysis does not make use of the system geometrical structure.

A different and less conservative way to study the effects of perturbations in LTI systems was made in (Kofman, 2002), whose main result will be applied here to study the properties of QSC.

4.1 Closed-Loop Equations

Consider the Continuous LTI plant (28) and controller (29).

$$\left\{ \begin{array}{rcl} \dot{x}_p(t) & = & A_p \cdot x_p(t) + B_p \cdot u_p(t) \\ y_p(t) & = & C_p \cdot x_p(t) \end{array} \right. \tag{28}$$

$$\left\{ \begin{array}{rcl} \dot{x}_c(t) & = & A_c \cdot x_c(t) + B_c \cdot u_c(t) + B_r \cdot u_r(t) \\ y_c(t) & = & C_c \cdot x_c(t) + D_c \cdot u_c(t) + D_r \cdot u_r(t) \end{array} \right. \tag{29}$$

With the interconnection given by (7), the following closed loop equation is obtained.

$$\dot{x}(t) = A \cdot x(t) + B \cdot u_r \tag{30}$$

where

$$x(t) = \left[\begin{array}{c} x_p(t) \\ x_c(t) \end{array} \right], \quad A = \left[\begin{array}{cc} A_p + B_p D_c C_p & B_p C_c \\ B_c C_p & A_c \end{array} \right]$$

and

$$B = \begin{bmatrix} B_p D_r \\ B_r \end{bmatrix}$$

The QSC implementation of the controller modifies (29) which can be rewritten as

$$\begin{cases} \dot{x}_c &= A_c \cdot q_c + B_c \cdot u_c + B_r \cdot u_r \\ y_c &= C_c \cdot q_c + D_c \cdot u_c + D_r \cdot u_r \end{cases} \tag{31}$$

As in the general case, the effects of the A/D and D/A asynchronous converters is given by (9). Thus, taking into account that equation, (28), (31) and the definition of the perturbation variables (11), the use of the QSC scheme transforms equation (30) into

$$\dot{x} = A(x + \Delta x) + F \cdot \Delta y + B \cdot u_r \tag{32}$$

where x, Δx and Δy have the same definition than in Eq.(13) and

$$F = \begin{bmatrix} B_p D_c & B_p \\ B_c & 0 \end{bmatrix} \tag{33}$$

4.2 Error in LTI QSC

Let $x(t)$ and $\tilde{x}(t)$ and be solutions of (30) and (32) starting from the same initial condition $x(t_0) = \tilde{x}(t_0) = x_0$. Then the error

$$e(t) = \tilde{x}(t) - x(t) \tag{34}$$

can be seen as a bound for the lost of performance due to the QSC implementation.

From (30), (32), (34) and the definitions of $x(t)$ and $\tilde{x}(t)$ we have

$$\begin{aligned} \dot{e}(t) &= A \cdot (e(t) + \Delta x(t)) + F \cdot \Delta y(t) \\ e(t_0) &= 0 \end{aligned}$$

Since the components of Δx and Δy are bounded by the corresponding quantum size adopted, Theorem 1 of (Kofman, 2002) can be applied in order to quantify the error due to the QSC scheme.

Theorem 2. *Let $x(t)$ and $\tilde{x}(t)$ be trajectories of a LTI CCS and its QSC implementation starting from the same initial condition and let A be the evolution matrix of the continuous closed loop system. If A is Hurwitz and diagonalizable, the difference between both trajectories is always bounded by*

$$|\tilde{x}(t) - x(t)| \leq |V|(|\mathbb{R}e(\Lambda)^{-1}\Lambda||V^{-1}|\Delta q_x + |\mathbb{R}e(\Lambda)^{-1}V^{-1}F|\Delta q_y) \tag{35}$$

where[2] *Δq_x is the vector of quantum sizes in the plant and controller state variables (all the components corresponding to the plant are zero), Δq_y is the vector of quantum sizes in the plant and controller output variables (introduced by the A/D and D/A converters respectively), the matrix F is defined according to* (33)*, Λ is a diagonal matrix of eigenvalues of A and V is a corresponding matrix of eigenvectors.*

The proof is straightforward using the mentioned theorem. Inequality (35) can be used as a design formula to obtain the quantization in the controller and converters according to the deviation allowed from the CCS trajectories.

A very important remark is that the mentioned bound does not depend on the initial condition or in the reference trajectory ($u_r(t)$). The only restriction is that $u_r(t)$ must be piecewise constant in order to guarantee that the QSC can be exactly represented by a DEVS model and then implemented on a digital device.

Theorem 2 says that the difference between the closed loop CCS trajectories and the corresponding QSC are always bounded. In that way, if the original continuous controller ensures asymptotic stability, its QSC implementation ensures ultimately boundedness for any quantization adopted.

Moreover, the bound stands for all t and this fact can produce an important improvement in the dynamic response with respect to discrete time approximations.

The closed form of Inequality (35) gives also a useful tool for the design of the quantization. The design procedure then consists just in choosing the maximum allowed error in each variable and then in finding the appropriate values of Δq_x and Δq_y to satisfy the inequality.

[2] *The symbol $|\cdot|$ denotes the componentwise modulus of a vector or matrix. For two vectors of the same dimension a and b, we say $a \leq b$ if the inequality stands for all their components. This implies that* (35) *expresses a bound for each state variable*

5 Examples

5.1 A PI controller example

Consider the plant (28) with

$$A_p = \begin{bmatrix} 0 & 1 \\ -1 & -4 \end{bmatrix}, B_p = \begin{bmatrix} 0 \\ 1 \end{bmatrix}, C_p = \begin{bmatrix} 1 & 0 \end{bmatrix} \tag{36}$$

A PI controller with parameters K_P and K_I can be written in the form of (29) with $A_c = 0$, $B_c = -1$, $B_r = 1$, $C_c = K_I$, $D_c = -K_P$ and $D_r = K_P$. Thus, using $K_P = K_I = 10$, the closed loop evolution matrix is

$$A = \begin{bmatrix} 0 & 1 & 0 \\ -11 & -4 & 10 \\ -1 & 0 & 0 \end{bmatrix}$$

A possible matrix of eigenvectors (calculated with Matlab) is

$$V = \begin{bmatrix} 0.0085 + j0.342 & 0.0085 - j0.342 & 0.5452 \\ -0.825 - j0.433 & -0.825 + j0.433 & -0.734 \\ -0.108 + j0.064 & -0.108 - j0.064 & 0.4049 \end{bmatrix}$$

Taking $\Delta q_c = \Delta y_p = 0.01$ and $\Delta y_c = 0.1$, the error bound according to (35) is 0.1443, 0.3383 and 0.0679 in each state variable of the plant and controller respectively. Thus, the maximum error on the plant oputput is bounded by 0.1443. Figure 3 shows the evolution of the plant output with the continuous controller and the QSC controller when the reference is a step of amplitude 10. Figure 4 shows the difference between both trajectories. The maximum difference was 0.1399 which is near the theoretical bound.

[Figure 3 about here.]

[Figure 4 about here.]

5.2 An inverted pendulum control

The model of the plant and the design of the continuous controller of this example were taken from (Messner and Tilbury, 1998).

Consider the inverted pendulum of Figure 5

[Figure 5 about here.]

Using parameters $M = 0.5$; $m = 0.2$; $b = 0.1$ (friction of the cart); $J = 0.006$; $g = 9.8$; and $l = 0.3$ (length to pendulum center of mass), a linearized model around $\theta = \pi$ is given by the equations:

$$\begin{bmatrix} \dot{x} \\ \ddot{x} \\ \dot{\Phi} \\ \ddot{\Phi} \end{bmatrix} = \begin{bmatrix} 0 & 1 & 0 & 0 \\ 0 & -0.181 & 2.672 & 0 \\ 0 & 0 & 0 & 1 \\ 0 & -0.454 & 31.18 & 0 \end{bmatrix} \begin{bmatrix} x \\ \dot{x} \\ \Phi \\ \dot{\Phi} \end{bmatrix} + \begin{bmatrix} 0 \\ 1.818 \\ 0 \\ 4.545 \end{bmatrix} u$$

where $\Phi \triangleq \theta - \pi$ is the deviation angle from the vertical position.

The goal is to implement a control for the cart position. The variables measured are x and Φ. Thus, the plant output equations can be written as

$$y = \begin{bmatrix} 1 & 0 & 0 & 0 \\ 0 & 0 & 1 & 0 \end{bmatrix} \begin{bmatrix} x \\ \dot{x} \\ \Phi \\ \dot{\Phi} \end{bmatrix}$$

Following a LQR design with weights $w_x = 5000$ and $w_\Phi = 100$ and then using a full state observer with estimator poles placed at $p_1 = 40$, $p_2 = 41$, $p_3 = 42$ and $p_4 = 43$ the resulting controller can be written in the form of (29), where

$$A_c = \begin{bmatrix} -82.64 & 1 & 1.037 & 0 \\ -1570 & 68.61 & 148.9 & -38.04 \\ 1.385 & 0 & -83.18 & 1 \\ 397.6 & 171.5 & 2209 & -95.11 \end{bmatrix}$$

$$B_c = \begin{bmatrix} 82.64 & -1.037 \\ 1699 & -40.22 \\ -1.385 & 83.18 \\ -76.18 & 1760 \end{bmatrix}; B_r = \begin{bmatrix} 0 \\ -128.6 \\ 0 \\ -3.214 \end{bmatrix}$$

$$Cc = \begin{bmatrix} 70.71 & 37.83 & -1055 & -20.92 \end{bmatrix}$$

and

$$Dc = \begin{bmatrix} 0 & 0 \end{bmatrix}; Dr = -70.71$$

For the QSC digital implementation of the controller, the following quantization sizes were adopted:

$$\Delta q_x = \begin{bmatrix} 0.001 \\ 0.015 \\ 0.002 \\ 0.04 \end{bmatrix}; \Delta q_y = \begin{bmatrix} 0.002 \\ 0.004 \\ 2 \end{bmatrix}$$

The QSC performance was compared with a classic discrete controller obtained from the discretization of the continuous controller. The sampling time of the classic digital controller was taken as $T_s = 0.01$. In this case, we also considered the presence of A/D and D/A converters with the same quantization than in the QSC control (i.e. 0.002 in the position, 0.004 in the angle and 2 in the controller output).

Figures 6-8 show the trajectories obtained with the continuous time controller (without quantization), with the QSC controller and the classic discrete time controller.

[Figure 6 about here.]

[Figure 7 about here.]

[Figure 8 about here.]

The first observation is that the QSC shows a much better performance during the transient (see Figure 7) and it reduces the final oscillations.

The number of A/D conversions performed by the QSC converters in the 5 seconds of simulation was 211 and 185 in the position and angle respectively while the classic digital controller performs $5/0.01 = 500$ conversions in each variable. Similarly, the number of D/A conversions in the QSC control was 303. The classic discrete time controller also performs 500 D/A conversions.

If we take into account what happens from $t = 3$ to $t = 5$ (during the *steady state*), we can see that the QSC only performs 29 A/D conversions in the postition, 44 A/D conversions in the angle and 76 D/A conversions while the discrete time controller performs 200 conversions in each variable. The reduction of the computational costs is evident.

These advantages are paid with more calculations at the controller (the number of changes in the internal variables is 1600 against the 500 in the discrete time controller). However, the time required to perform A/D and D/A conversions is always much bigger than the time used for a simple calculation. Anyway, the number of calculations at the controller can be also reduced using a different realization. An interesting alternative is to use a diagonal –or block-diagonal– evolution matrix A_c. In this way, the QSS simulation becomes much more efficient. In one hand, the number of changes in the quantized variables is reduced. In the other hand, each transition involves calculations only in the state which is actually changing (one of the most important features of QSS simulation is that it exploits the sparsity properties). In our example, the use of a block diagonal controller reduces the number of calculations to 547 in 5 seconds obtaining a similar performance.

It is also interesting to observe that the fastest pole of the closed-loop system is placed at 43. Thus, the mean sampling frequencies in the QSC during the *steady state* are below the system bandwidth. Thus, the QSC scheme works violating the Nyquist frequency. It is well known that a sampled data system working below that frequency will be unstable. QSC can work using that frequency because the equilibrium point in the QSC scheme is in fact unstable (but the solutions are ultimately bounded).

Finally, it should be mentioned that the use of inequality (35) gives a quite conservative bound in this case. The error bound in $x(t)$ is 3.08, which is about 300 times bigger than the error observed in Figure 6. Anyway, a Lyapunov analysis gives a bound of 9.6×10^9, which is completely useless for the design.

5.3 A time varying example

The unstable time varying plant

$$\begin{cases} \dot{x}_p &= x_p \cdot (1 + \sin t + \cos t) + u_p \\ y_p &= (2 + \cos t) \cdot x_p \end{cases} \tag{37}$$

can be stabilized by the controller

$$\begin{cases} \dot{x}_c &= -x_c + u_c \\ y_c &= -x_c - u_c \end{cases} \tag{38}$$

The resulting closed loop system can be written as

$$\begin{cases} \dot{x}_p &= -(1-\sin t)\cdot x_p - x_c \\ \dot{x}_c &= (2+\cos t)\cdot x_p - x_c \end{cases} \tag{39}$$

Here, the Lyapunov candidate

$$V(x_p, x_c, t) = x_p^2 + \frac{1}{2}x_c^2 + \frac{1}{2}x_p^2\cos t \tag{40}$$

verifies (15) with

$$W_1(x_p, x_c) = \frac{1}{2}x_p^2 + \frac{1}{2}x_c^2 \tag{41}$$

$$W_2(x_p, x_c) = \frac{3}{2}x_p^2 + \frac{1}{2}x_c^2 \tag{42}$$

The orbital derivative is

$$\frac{\partial V}{\partial x}\cdot f(x,t) + \frac{\partial V}{\partial t} = (2+\cos t)\cdot(\sin t - 1)\cdot x_p^2 - x_c^2 - \frac{1}{2}x_p^2\sin t \tag{43}$$

which satisfies (16) with

$$W_3 = -\frac{1}{2}x_p^2 - x_c^2 \tag{44}$$

Then, the closed loop CCS is asymptotically stable and the algorithm resulting from Theorem 1 can be used to design the QSC controller.

The first step for the QSC design consists in choosing the region of attraction and the ultimate bound. Since inequalities (15)–(16) stand in $\Re^2$ (i.e. the CCS stability is global) it is not necessary to restrict the region of attraction except for chosing the saturation values. In this case, the choice of Ω_{2_a} does not affect the calculations.

The ultimate bound Ω_{1_b} will be chosen with $b = 0.5$. Then, taking into account (41) it results that $\Omega_{1_b} = \{x \in \Re^2 | \|x\| \leq 1\}$.

The perturbed equations (13) can be written as

$$\begin{cases} \dot{x}_p &= -(1-\sin t)\cdot x_p - x_c - \Delta x_c + \Delta y_c - \Delta y_p \\ \dot{x}_c &= (2+\cos t)\cdot x_p - x_c - \Delta x_c + \Delta y_p \end{cases} \tag{45}$$

and then, from (20) function $\alpha(x, \Delta x, \Delta y, t)$ results

$$\alpha = -x_c^2 - \frac{1}{2}x_p^2 + x_p\cdot(2+\cos t)\cdot(-\Delta x_c + \Delta y_c - \Delta y_p) + x_c\cdot(-\Delta x_c + \Delta y_p) \tag{46}$$

Although the maximum α_M in (22) cannot be easily obtained, it can be bounded as follows

$$\begin{aligned} \alpha &\leq -\frac{1}{2}\|x\|^2 + \sqrt{9\cdot(|\Delta x_c|+|\Delta y_c|+|\Delta y_p|)^2+(|\Delta x_c|+|\Delta y_p|)^2}\cdot\|x\| \\ &\leq \|x\|\cdot(-\frac{1}{2}\|x\| + \sqrt{9\cdot(|\Delta x_c|+|\Delta y_c|+|\Delta y_p|)^2+(|\Delta x_c|+|\Delta y_p|)^2}) \end{aligned}$$

and then, taking into account that $\|x\| > 1/3$ in $\Omega_{1,2}$, it results that

$$\alpha_M \leq -\frac{1}{18} + \sqrt{(|\Delta x_c|+|\Delta y_c|+|\Delta y_p|)^2+\frac{1}{9}(|\Delta x_c|+|\Delta y_p|)^2}$$

Then, taking the quantum equal to 0.018 in the controller and converters we can ensure that

$$\alpha_M \leq -0.0093 \tag{47}$$

in $\Omega_{1,2}$, which implies that the trajectories finish inside Ω_{1_b} in finite time, with a minimum *speed* $s_1 = 0.0093$.

Figures 9–14 show the simulation results for an initial condition $x_p = 5$, $x_c = 0$.

[Figure 9 about here.]

[Figure 10 about here.]

[Figure 11 about here.]

[Figure 12 about here.]

[Figure 13 about here.]

[Figure 14 about here.]

Figure 14 also shows that the design was very conservative. The ultimate bound observed in the simulation is less than 0.03 (in norm 2) which is more than 30 times smaller than the calculated.

There are two reasons which can explain this. The first one is just what was mentioned above: Lyapunov analysis often leads to conservative estimations of the ultimate bound. The second reason is that in this case the D/A converter does not introduce any perturbation since it is exactly matched with the quantizer of x_c and the A/D converter.

This last fact can be easily observed in the output equation of system (38), which in QSC adopts the form of

$$y_c = -q_c - u_c \tag{48}$$

and then, if the quantization levels of q_c and the A/D converter coincide with the quantization levels of the D/A converter the effect of this last converter can be ignored since y_c can only adopt exactly the quantized values.

This fact constitutes another advantage of QSC since the correct matching can eliminate the quantization effects of the D/A converters.

6 Conclusions

Quantized State Control is an alternative way to implement digital controllers designed in continuous time. Its most remarkable feature is the avoidance of time discretization which results in an important improvement of the implementation stability properties.

Other interesting advantage is the reduction of the computational costs as a result of the asynchronous sampling scheme. Here, the converters only take samples when it is necessary (i.e. when they differ from the previous value in a given quantity). Similarly, the controller internal states are recalculated under the same condition. Thus, QSC can be thought as a control strategy which only acts when it has to.

The way in which QSC is implemented allows its representation as a perturbed version of the original continuous control system. Based on previous results on perturbartion analysis not only stability but also error bound properties were proven. Those properties –which were studied for general nonlinear time varying plants and also particularized for LTI cases– can be also used in a practical sense for design purposes.

As it was already mentioned the design of QSC consists just in choosing the quantum to be used in the controller state variables and converters. The algorithms and formulas derived from the perturbation analysis allow to make the choice so that stability and error bound properties are theoretically ensured.

Another fact which should be remarked is related to the information used by the QSC controller. Once the controller gets its first input value, the asynchronous A/D converters can transmit the following values using only one bit per conversion with the sign of the change. In a similar way –provided that there is some matching between the internal quantizers and converters– the controller outputs can be transmitted with only one bit each time. This is

a very important advantage in distributed control systems, where the information has to be transmitted between sensors, controllers and actuators. Although there are some results based on quantization to reduce the ammount of information (Elias and Mitter, 2001), the use of only one bit was never achieved with other non–trivial control schemes.

This work opens many problems which should be treated in the future. From the practical point of view, it is important to study the effects of the delays introduced by the implementation on the stability properties. That study should also include a characterization of the delays which would require some experimental work in real applications.

When it comes to theoretical aspects, the most important properties were proven for general nonlinear time varying systems and for LTI systems. There is an intermediate case which should be taken into account which corresponds to Linear Parameter–Varying (LPV) plants. The example of Section 5.3 in fact corresponds to that category and although a Lyapunov analysis could be done for that case, the result was very conservative. If the geometrical analysis for LTI systems in Section 4 were extended for LPV plants, less conservative results might be obtained.

It is also important to study the way in which QSC affects not only the stability, region of attraction and error bound but also other performance measures (mean square error, overshoot, etc.).

Finally, it should be mentioned that QSS are just a small class of the wide family of DEVS models. The possibility of obtaining different DEVS models which can act as asynchronous controllers with nice stability properties must be also taken into account.

References

Brockett, R. and Liberzon, D. (2000). Quantized feedback stabilization of linear systems. *IEEE Trans. Automat. Contr.*, 45:1279–1289.

Delchamps, D. (1990). Stabilizing a linear system with quantized state feedback. *IEEE Trans. Automat. Contr.*, 35:916–924.

Elias, N. and Mitter, S. (2001). Stabilization of Linear Systems with Limited Information. *IEEE Trans. Automat. Contr.*, 46(9):1384–1400.

Farrel, J. and Michel, A. (1989). Estimates of asymptotic trajectory bounds in digital implementations of linear feedback control systems. *IEEE Trans. Automat. Contr.*, 34:1319–1324.

Hou, L., Michel, A., and Ye, H. (1997). Some qualitative properties of sampled-data control systems. *IEEE Trans. Automat. Contr.*, 42:1721–1725.

Hu, L. and Michel, A. (1999). Some qualitative properties of multirate digital control systems. *IEEE Trans. Automat. Contr.*, 44:765–770.

Khalil, H. (1996). *Nonlinear Systems.* Prentice-Hall, New Jersey, 2nd edition.

Kofman, E. (2001). Quantized-State Control. A Method for Discrete Event Control of Continuous Systems. Technical Report LSD0105, LSD-UNR. To appear in *Latin American Applied Research* Journal. Available at www.eie.fceia.unr.edu.ar/∼ekofman/.

Kofman, E. (2002). Non Conservative Ultimate Bound Estimation in LTI Perturbed Systems. In *Proceedings of AADECA 2002*, Buenos Aires, Argentina.

Kofman, E. and Junco, S. (2001). Quantized State Systems. A DEVS Approach for Continuous System Simulation. *Transactions of SCS*, 18(3):123–132.

Lunze, J., Nixdorf, B., and Schrder, J. (1999). Deterministic Discrete-Event Representations of Linear Continuous–Variable Systems. *Automatica*, 35(3):395–406.

Messner, W. and Tilbury, D. (1998). *Control Tutorials For MATLAB And Simulink: A Web-Based Approach.* Addison-Wesley.

Miller, R., Michel, A., and Farrel, J. (1989). Quantizer effects on steady-state error specifications of digital feedback control systems. *IEEE Trans. Automat. Contr.*, 34:651–654.

Miller, R., Mousa, M., and Michel, A. (1988). Quantization and overflow effects in digital implementation of linear dynamic controllers. *IEEE Trans. Automat. Contr.*, 33:698–704.

Sayiner, N., Sorensen, H., and Viswanathan, T. (1993). A non-uniform sampling technique for A/D conversion. In *Proceedings of ISCAS'93*, volume 2, pages 1220–1223.

Zeigler, B. and Kim, J. (1993). Extending the DEVS-Scheme knowledge-based simulation environment for real time event-based control. *IEEE Trans. on Robotics and Automation*, 3(9):351–356.

Zeigler, B., Kim, T., and Praehofer, H. (2000). *Theory of Modeling and Simulation. Second edition.* Academic Press, New York.

Zeigler, B. and Lee, J. (1998). Theory of quantized systems: formal basis for DEVS/HLA distributed simulation environment. In *SPIE Proceedings*, pages 49–58.

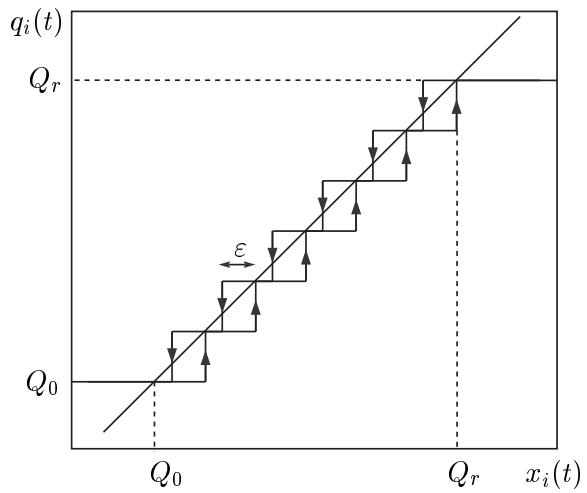

Figure 1: Quantization Function with Hysteresis

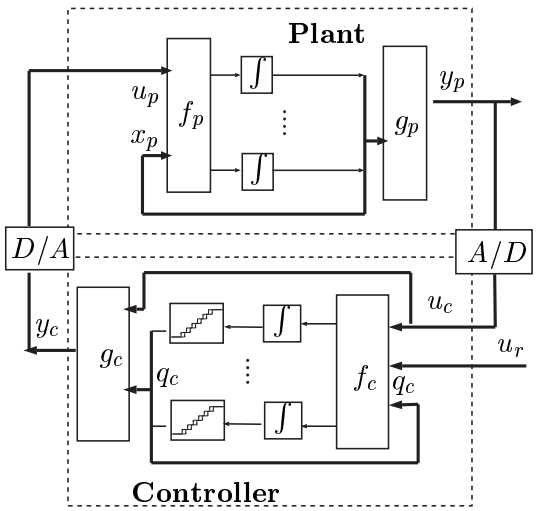

Figure 2: Block Diagram of the QSC system

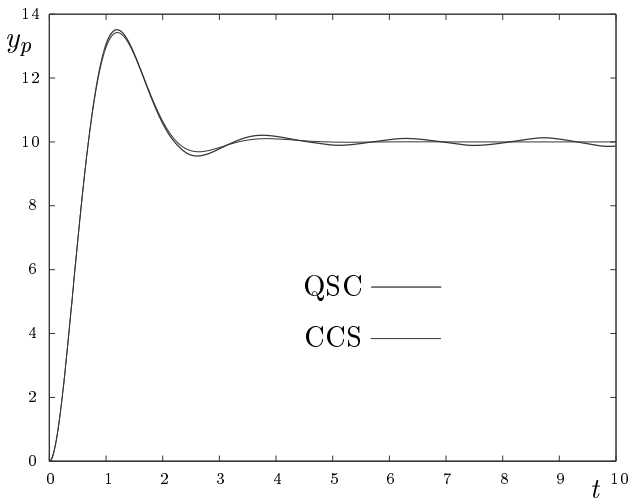

Figure 3: Plant output with CCS and QSC

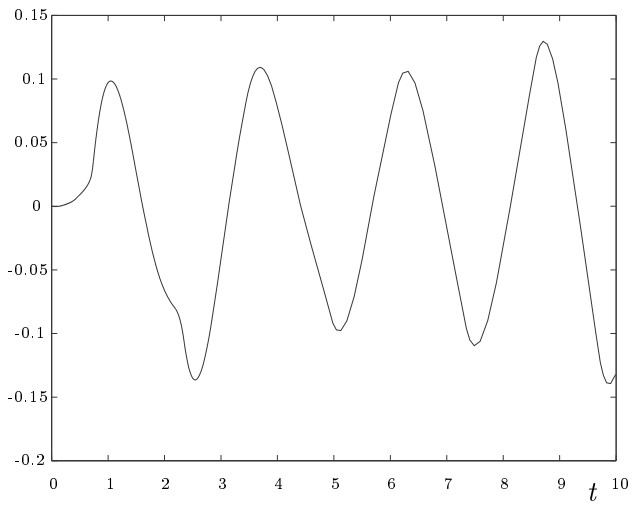

Figure 4: Difference in the plant output with CCS and QSC

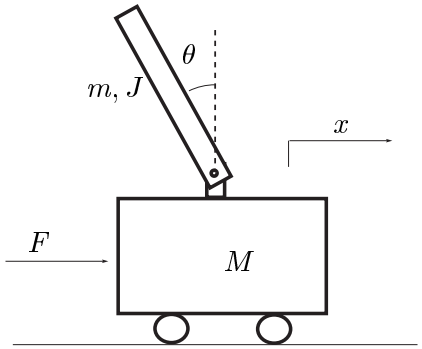

Figure 5: Inverted Pendulum scheme

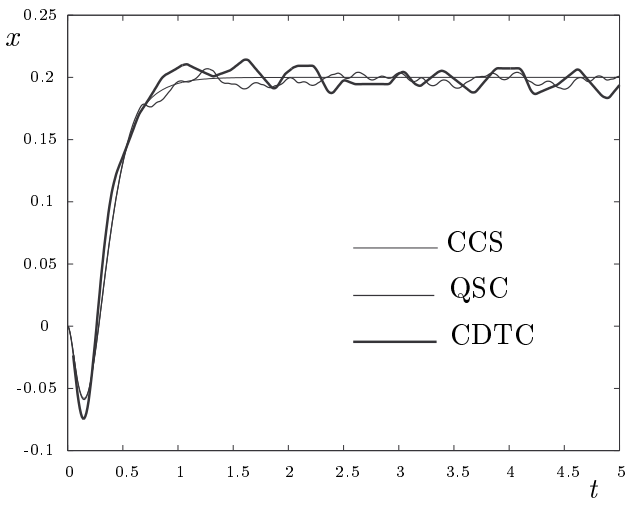

Figure 6: Cart position with QSC and Classic Digital Control.

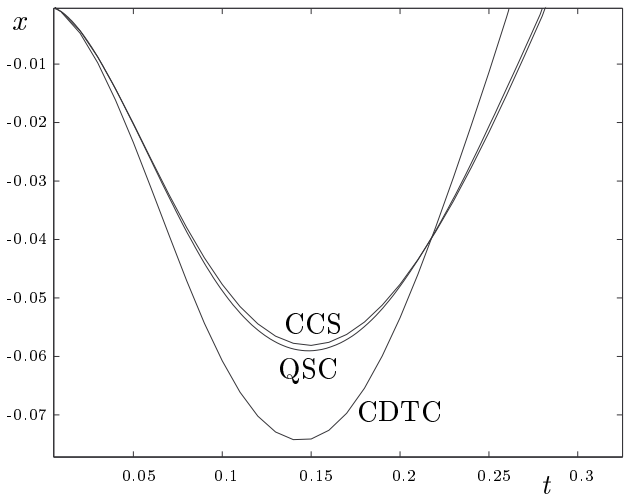

Figure 7: Cart position (start up) with QSC and Classic Digital Control.

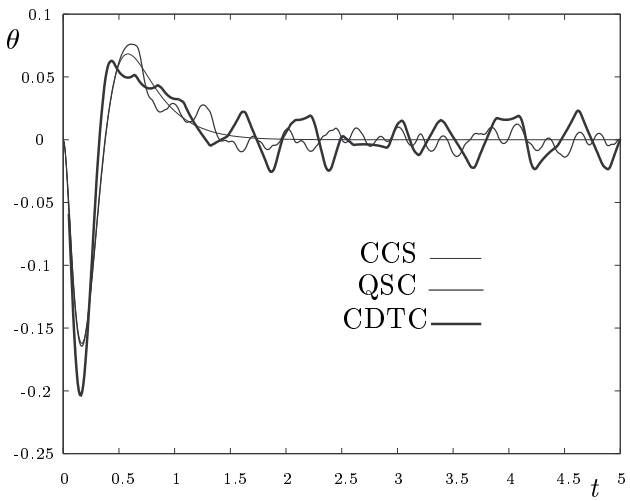

Figure 8: Pendulum angle with QSC and Classic Digital Control.

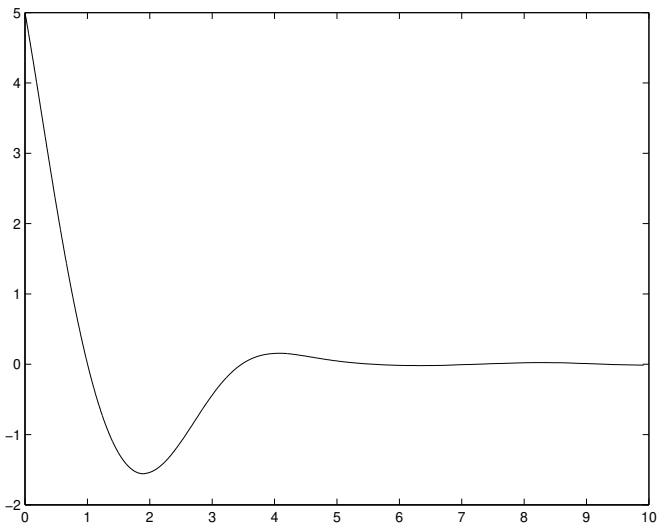

Figure 9: x_p vs. t

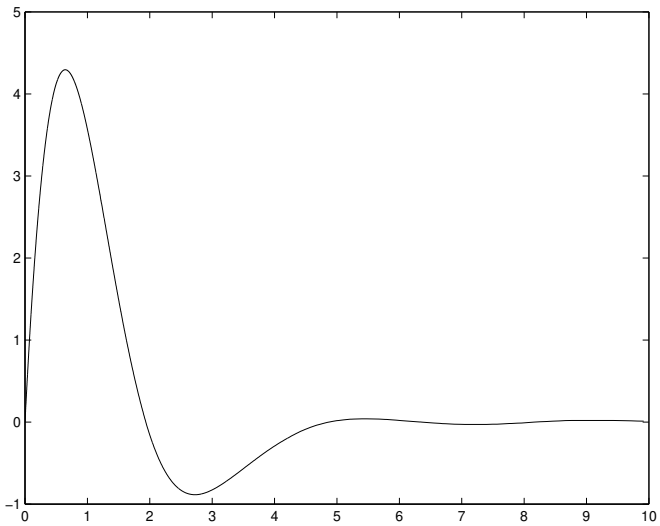

Figure 10: x_c vs. t

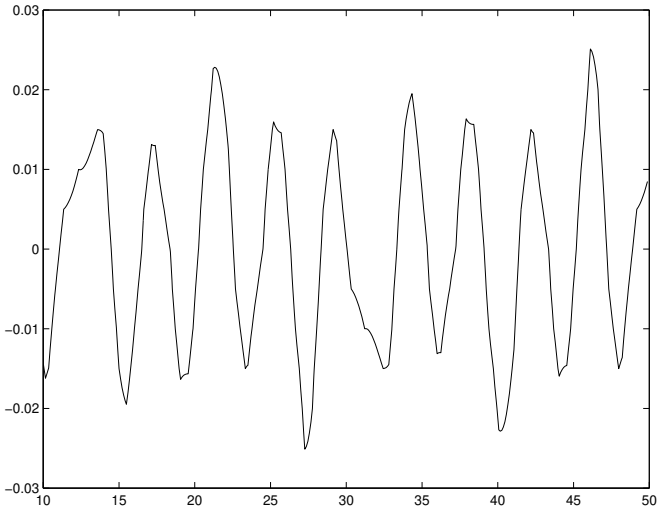

Figure 11: Final oscillations in x_p vs. t

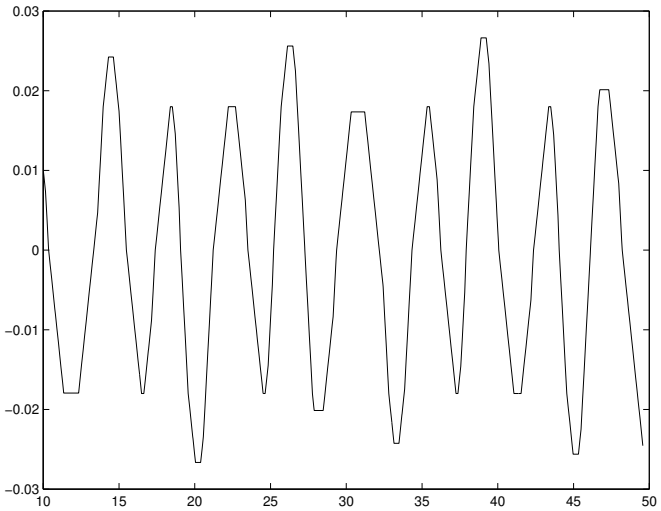

Figure 12: Final oscillations in x_c vs. t

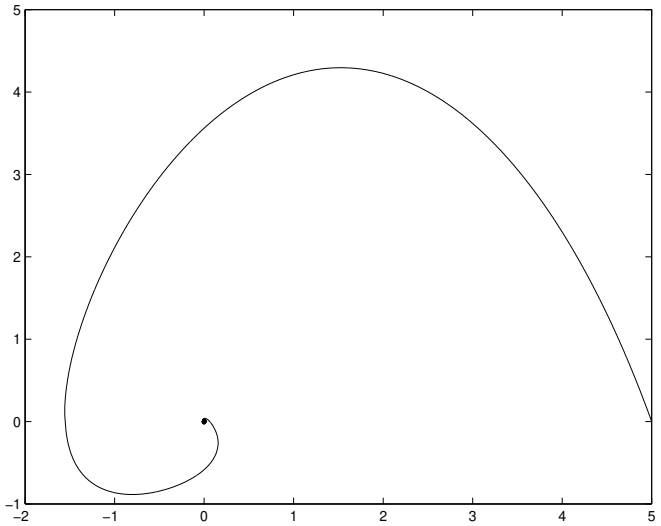

Figure 13: x_p vs. x_c

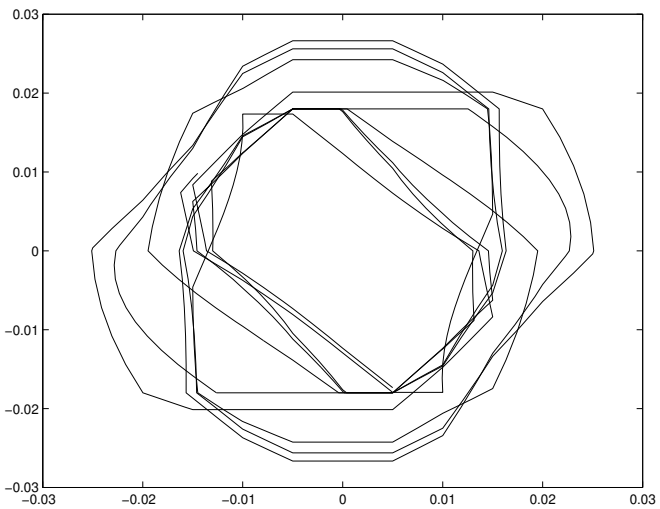

Figure 14: Final oscillations in x_p vs. x_c